OPEN ACCESS
IOP Publishing | ISECAEP
Journal of Reliability Science and Engineering
J. Reliab. Sci. Eng. **2** (2026) 025102 (14pp)
https://doi.org/10.1088/3050-2454/ae6594

Accuracy stability comprehensive evaluation of meta-action unit in CNC machine tools

Jindong Xu[1], **Yan Ran**[1,*] **and Ke Tian**[2]

[1] State Key Laboratory of Mechanical Transmission for Advanced Equipment, Chongqing University, Chongqing 400044, People's Republic of China
[2] China North Industries Group Corporation Limited, Beijing 10053, People's Republic of China

E-mail: ranyan@cqu.edu.cn

Received 19 January 2026, revised 8 April 2026
Accepted for publication 28 April 2026
Published 8 May 2026

Abstract

To address the shortcomings in the evaluation of precision stability of CNC machine tools, this paper takes the element action unit as the object, analyzes four types of fluctuation mechanisms such as wear, establishes four precision fluctuation models, and proposes accuracy fluctuation rate, accuracy variation rate, accuracy variation coefficient, accuracy stability coefficient (ASC), and comprehensive index accuracy stability index (ASI). In the worm gear rotation unit test, when the torque is 1–24 N m, ASC decreases from 7.88 to 3.15, and ASI increases from 0.0357 to 0.181; When the ASI exceeds the threshold of 0.1, abnormal accuracy is determined. This system effectively quantifies accuracy fluctuations and identifies anomalies, providing reference for accuracy stability evaluation.

Keywords: accuracy stability, accuracy fluctuation, kinematic error, evaluation indicator

1. Introduction

The accuracy stability, as a critical indicator for the development level of CNC machine tools, has gradually gained importance to improve it in recent years with the demands of technological innovation and industrial upgrading. However, research on the accuracy stability of CNC machine tools started relatively late both domestically and internationally. In terms of accuracy calculation and evaluation methods, Ran and Lv [1] proposed a two-stage gray cloud model to evaluate the abnormal degree of workpiece machining accuracy, integrating ARIMA-SPC for outlier detection, Markov transition matrix for credibility assessment, and cloud-AHP combined with entropy weight method for comprehensive weighting; Liu and Li [2] built a thermal error model based on Cpk-selected temperature points, significantly enhancing the process capability index. In terms of structural improvement and error compensation, Chao and Li [3] analyzed geometric error types of five-axis CNC machine tools, proposed a modeling method based on multi-body system theory and homogeneous coordinate transformation, and compared offline detection and online real-time compensation techniques to significantly improve spatial positioning accuracy; Song *et al* [4] implemented real-time compensation for time-varying errors in CNC machine tools based on TCP/IP protocol, improving the stability of machine tool accuracy. In terms of model construction and prediction, Mechta *et al* [5] assessed the correlation between intra-axis errors of prismatic axes and proposed Bézier and B-spline models as flexible alternatives to polynomials for modeling these errors, achieving residuals within machine repeatability on three CNC machine tools with different controllers and guidance technologies; Chen *et al* [6] proposed a method for predicting assembly accuracy stability based on contact pressure distribution entropy; He *et al* [7] analyzed the impact of assembly errors on accuracy stability through methods such as homogeneous coordinate

* Author to whom any correspondence should be addressed.

Original content from this work may be used under the terms of the Creative Commons Attribution 4.0 licence. Any further distribution of this work must maintain attribution to the author(s) and the title of the work, journal citation and DOI.

© 2026 The Author(s). Published by IOP Publishing Ltd on behalf of the Institute of Systems Engineering, China Academy of Engineering Physics

transformation. Additionally, Zhou [8] researched causes of machine tool accuracy instability and specific accuracy measurement adjustments for vertical lathes.

Since CNC machine tools are complex mechanical systems composed of multiple components and motion mechanisms, the traditional research methods often focus on the overall machine tool or large-scale motion modules. This approach makes it difficult to accurately trace the source of accuracy fluctuations. Moreover, the evaluation indexes established without considering meta-actions (MA) may not be able to reflect the essence of accuracy stability comprehensively and accurately, as they ignore the influence of basic motion units on the overall accuracy.

For these reasons, this paper takes MA unit (MAU) as the research object (treated as an independent motion unit [9, 10]). By analyzing fluctuation mechanisms for four typical causes of accuracy fluctuation, four corresponding models are derived. Subsequently, general rules of accuracy fluctuation are established, based on which relevant evaluation indexes are proposed, and an evaluation index system for MA units' accuracy stability is formed. Finally, a comprehensive evaluation of its accuracy stability (based on the system) is presented, along with explanations for identifying precision anomalies in such units.

2. Kinematic error (KE) model based on MA theory

The core of the MA theoretical system is a dynamic structured decomposition method based on 'function-motion-action (FMA)' [11, 12]. As a top-down, layer-by-layer approach, FMA breaks down the mechanical transmission systems of complex electromechanical products into three layers: Function (F), Motion (M), and Action (A). In this system, MA—components of the action layer—are performed by the interaction of multiple parts assembled in specific ways. Since the functions and performance of CNC machine tools depend primarily on the relative motion of their parts during operation, parts analysis must be integrated into FMA decomposition to examine transmission system state changes. This forms the 'function-motion-action-part (FMAP)' structured decomposition method, as shown in figure 1.

As shown in figure 1, the motion layer refers to the level of movement or movement combination of components, ensuring the normal realization of a specific function in the functional layer. The action layer refers to the level of actions or action combinations, guaranteeing the normal completion of a specific movement in the motion layer. The part layer refers to the level of parts or part combinations, enabling the normal completion of a certain action in the action layer.

MA and MAU are inseparable: MA is the motion manifestation of the MAU, while the MAU is the carrier for MA execution. Even complex mechanical transmission systems can be decomposed into MA, so the operational state of MA directly or indirectly determines a product's function and performance. Focusing on MA to study quality characteristics (e.g. accuracy, reliability) of CNC transmission systems simplifies analysis significantly.

The kinematic accuracy of a CNC machine tool's MA refers to the proximity between the actual and ideal motion trajectories of MAUs output elements during operation. Output elements here denote points, lines, or surfaces where the MAU's output part transmits power to the downstream MAU's input part (IE). Error is used as an indicator to evaluate accuracy. Therefore, the main factors that affect the kinematic accuracy of an MA, that is, KE, include the input error of the IE, the assembly error within the MAU (AE) and the geometric error of the output element of the output part (GE). The KE model of an MA is established, as shown in equation (1)

$$\mathrm{KE} = \mathrm{IE} + \mathrm{AE} + \mathrm{GE}. \tag{1}$$

According to the random error theory [13, 14], IE, AE, GE, and KE all obey normal distribution.

3. MAU accuracy fluctuation: mechanisms and models analysis

3.1. Typical accuracy fluctuation mechanisms

During the operation of CNC machine tools, accuracy fluctuation stems from multiple factors, generally falling into four main categories: wear, deformation, impurities, and vibration. Essentially, the root cause of such fluctuation lies in changes to the KE of the MA. KE is composed of three core components: IE, AE, and GE.

Wear is a prevalent cause of accuracy fluctuation in CNC machine tools. It occurs primarily between relatively moving surfaces within the MAU and mainly affects the MAU's AE. Based on surface damage mechanisms, wear is classified into three types [15], as shown in figure 2. Abrasive wear refers to surface material removal caused by friction between an object's surface and hard particles or micro-peaks on mating surfaces (figure 2(a)). Adhesive wear happens when sliding surfaces, under load, undergo local plastic deformation or shearing. Frictional heat leads to metal adhesion on the contact surface; during subsequent relative sliding, adhered metal chips peel off and transfer to another surface, causing part material loss (figure 2(b)). Surface fatigue wear involves material loss from relatively moving contact surfaces due to fatigue under cyclic contact pressure (figure 2(c)). These wear forms typically coexist.

Their impact on KE is realized by altering AE. When 'peak-clipping' wear occurs—meaning mating surfaces grow smoother—the upper deviation, expectation, and variance of part GE decrease, while the lower deviation remains unchanged. Since AE and KE have linear relationships with GE, their upper deviation, expectation, and variance also decrease, with the lower deviation unchanged. When 'pit-digging' wear occurs—making surface morphology irregular—the lower deviation and expectation of GE increase, while the upper deviation decreases. This leads to higher lower deviation and expectation of AE, and KE follows the same trend.

During CNC machine operation, granular substances such as dust and debris are inevitably encountered. When these

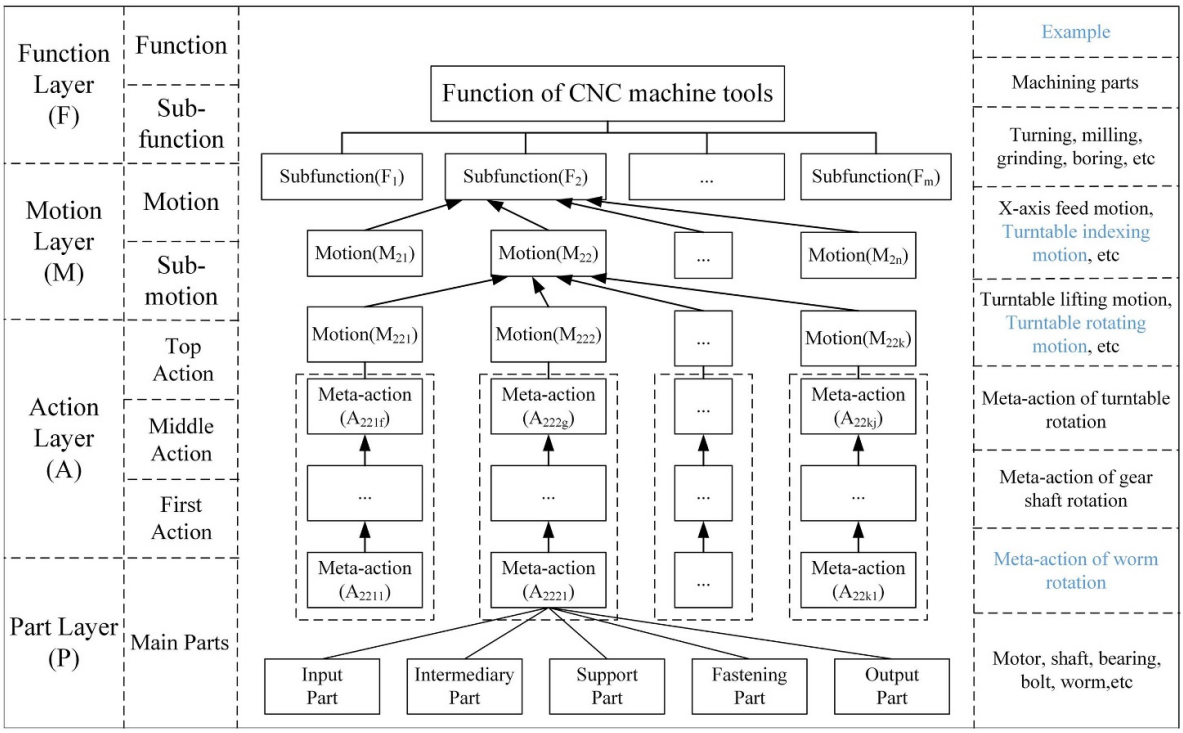


Figure 1. FMAP decomposition diagram.

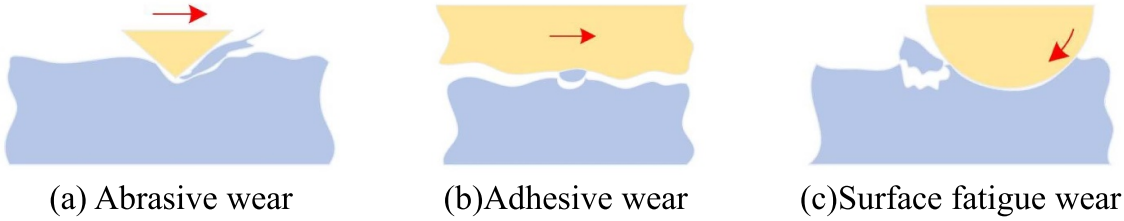


Figure 2. Schematic diagram of wear mechanism.

impurities enter the contact-fitting area of dynamic mating parts in the MAU, they alter AE without changing GE. Impurities are categorized by their volume relative to part surface troughs, as shown in figure 3.

When the volume of impurity particles is less than or equal to the volume of the surface troughs, particles fill the part surface troughs, reducing the fitting error's lower limit deviation (upper limit deviation remains unchanged). This increases the fitting error's expected value and decreases its variance, with the MAU's KE following the same trend as its AE. When the volume of the impurity particles is greater than the volume of the surface troughs, the particles will act as 'peaks' on the surface of the parts. In this case, the fitting error's upper limit deviation increases, and the original upper limit deviation becomes the new lower limit deviation. This raises the fitting error's expected value, with the MAU's KE changing alongside its AE.

During CNC machine operation, fluctuations in cutting force, ambient temperature, and frictional heat cause part deformation. This deformation affects both AE and GE. Based on deformation causes and locations, 12 fluctuation mechanisms exist, as shown in table 1. Among them, the mechanism of the effect of fitting surface deformation on fitting error is shown in figure 4.

In table 1, the deformation of the fitting surface only changes the morphology of the peaks on the surface of the part but not the shape and position of the troughs, whereas overall deformation of the part changes both the morphology and position of the surface peaks and troughs.

Temperature changes lead to uneven expansion of the fitting surface—troughs expand more than peaks. This increases the upper deviation and expectation of GE, while the lower deviation remains unchanged. In turn, the upper and lower deviations of fitting error between parts increase, as does the expectation. Ambient temperature changes or internal heat sources from part friction can alter the expected fitting error between components. Since the MAU's KE and AE have a linear relationship with fitting error, and temperature-induced part deformation is reversible, the MAU's KE fluctuates. Other deformation scenarios follow similar logic: for example,

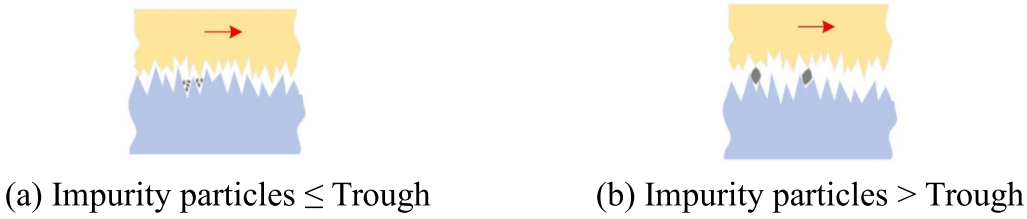


Figure 3. Mechanisms of impurity.

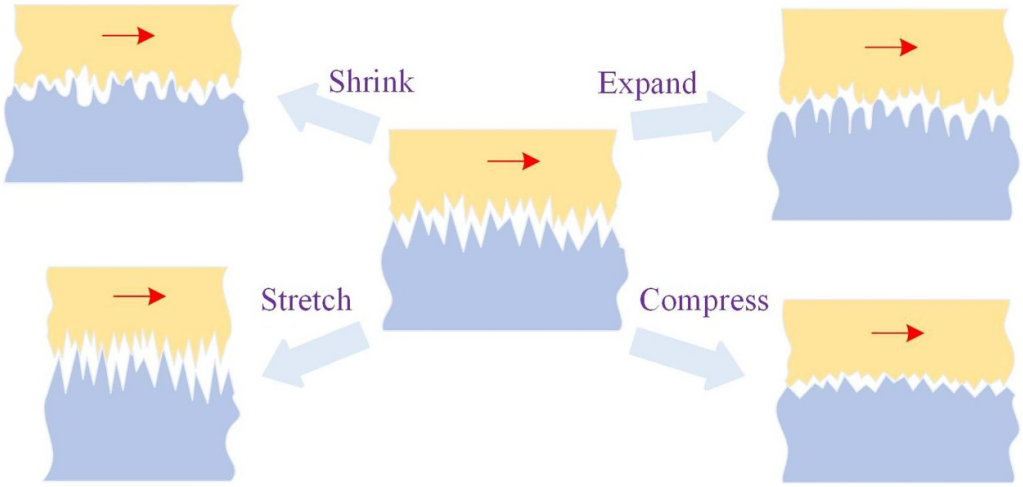


Figure 4. Deformation mechanism on the fitting surface.

Table 1. Mechanism of accuracy fluctuation caused by deformation.

Deformation form	Deformation area	Upper limit deviation	Lower limit deviation	Expectation
Expansion or stretching	Fitting surface	↑	↑	↑
	Whole part	↑	↑	↑
	Working surface	↑	—	↑
Shrinkage or compression	Fitting surface	↓	↓	↓
	Whole part	↓	↓	↓
	Working surface	↓	—	↓

'↑' represents increase; '↓' represents decrease; '-' represents no change.

shrinkage or compression of the whole part reduces the upper and lower deviations and expectation of GE, which then lowers the upper and lower deviations and expectation of AE and KE.

Vibration is unavoidable during CNC machine machining. For the MAU, vibration mainly affects AE in two ways, as shown in figure 5.

As shown in figure 5, when an MAU is subjected to vibration, components with a clearance-fit relationship will oscillate within these clearances. When oscillation aligns with vibration direction, the upper and lower deviations of AE increase, as does the expectation. When oscillation opposes vibration direction, these parameters decrease, and AE fluctuates with vibration amplitude within a cycle. For slippage in the fitting domain of the components' mating surfaces, the upper and lower limit deviations and the expected value of the AE all undergo changes. From equation (1), the KE of the MAU is proportional to the AE. Therefore, as long as the MAU is subject to vibration interference, its accuracy will fluctuate.

3.2. *Typical accuracy fluctuation models of MA units*

As previously analyzed, wear, impurity, deformation, and vibration can all cause changes in the upper and lower limit deviations, expected values, and variance of the KE in an MAU. Therefore, the typical accuracy fluctuation models of the MAU can be categorized into single-type accuracy fluctuation models and a composite-type accuracy fluctuation model. Here, the single-type precision fluctuation models include deviation-type, expectation-type, and variance-type accuracy fluctuation models, while the composite-type accuracy fluctuation model is a combination of deviation, expectation, and variance in accuracy fluctuation.

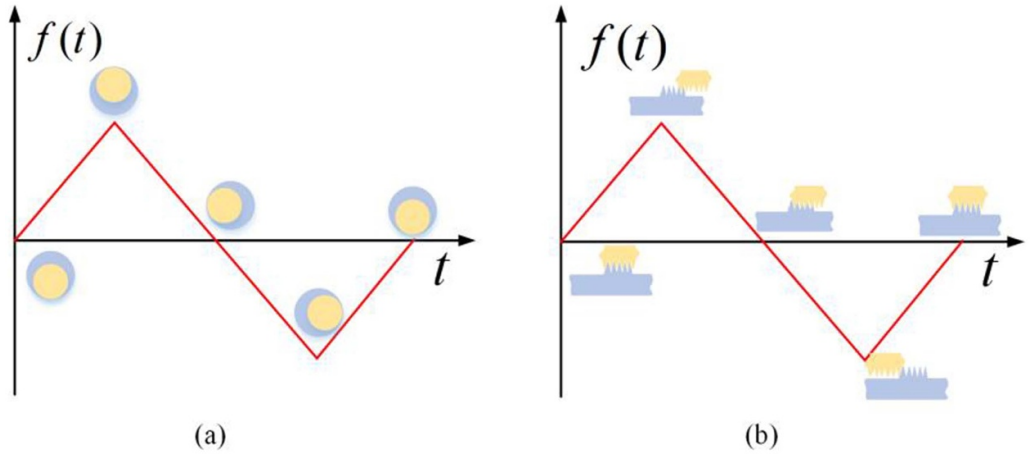


Figure 5. Schematic diagram of vibration mechanism. (a) Bounce, (b) slip.

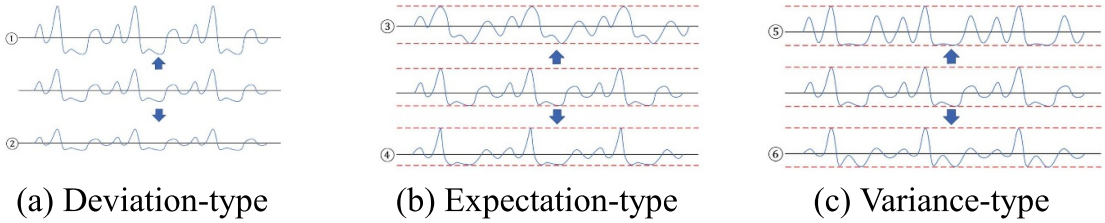


Figure 6. Schematic diagram of accuracy fluctuation.

(1) Deviation-type accuracy fluctuation model

The deviation-type accuracy fluctuation model refers to a model where the upper and lower limit deviations of the KE distribution of the MAU in CNC machine tools change, while the expectation and variance remain constant. As defined, the deviation-type accuracy fluctuation means that the KE is 'equally' distributed on both sides of its expectation; that is, the volume on both sides of the expectation as the dividing line is equal, as shown in figure 6(a).

In figure 6(a), there are many causes for the deviation-type accuracy fluctuation model ①, such as a combination of thermal expansion deformation, wear and vibration, or a combination of force-induced tensile deformation and vibration. Similarly, there are numerous causes for the deviation-type precision fluctuation model ②, such as a combination of thermal contraction deformation and vibration, or a combination of impurities, wear and vibration.

Take the limit deviation of the X-direction KE of the MAU as an example. From equation (1), it can be inferred that the X-direction KE of the MAU is

$$\mathrm{KE}_X = \mathrm{IE}_X + \mathrm{AE}_X + \mathrm{GE}_X. \tag{2}$$

Then its upper and lower limit deviations are

$$\begin{cases} T_{XU} = T_{\mathrm{I}XU} + T_{\mathrm{A}XU} + T_{\mathrm{G}XU} \\ T_{XL} = T_{\mathrm{I}XL} + T_{\mathrm{A}XL} + T_{\mathrm{G}XL} \end{cases}. \tag{3}$$

When the MAU occurs in a deviation-type accuracy fluctuation, the limit deviation of the X-direction KE satisfies equation (4).

$$\begin{aligned} T'_{\mathrm{XU}} &= \zeta_{\mathrm{XU}} T_{\mathrm{XU}} = \zeta_{\mathrm{IXU}} T_{\mathrm{IXU}} + \zeta_{\mathrm{AXU}} T_{\mathrm{AXU}} + \zeta_{\mathrm{GXU}} T_{\mathrm{GXU}} \\ T'_{\mathrm{XL}} &= \zeta_{\mathrm{XL}} T_{\mathrm{XL}} = \zeta_{\mathrm{IXL}} T_{\mathrm{IXL}} + \zeta_{\mathrm{AXL}} T_{\mathrm{AXL}} + \zeta_{\mathrm{GXL}} T_{\mathrm{GXL}} \end{aligned}. \tag{4}$$

In the equation (4), ζ_{XU} and ζ_{XL} respectively represent the fluctuation factor of the upper and lower limit deviations of the X-direction KE when the MAU fluctuates; ζ_{IXU}, ζ_{AXU} and ζ_{GXU} respectively represent the fluctuation factor of the upper limit deviation of the X-direction IE, AE, and GE; ζ_{IXL}, ζ_{AXL} and ζ_{GXL} respectively represent the fluctuation factor of the lower limit deviations of the IE, AE, and GE.

(2) Expectation-type accuracy fluctuation model

The expectation-type accuracy fluctuation model refers to a model in which the limit deviations and variance of the KE distribution of the MAU in CNC machine tools remain unchanged, with only the expectation varying. As defined, the expectation-type accuracy fluctuation means that the KE, bounded by the upper and lower limit deviations, maintains its basic waveform, with differences occurring at non-characteristic parts of the waveform, leading to the movement of the volume bisector line up or down, as shown in figure 6(b).

In figure 6(b), many factors can cause the expectation-type accuracy fluctuation model ③, such as a combination of thermal expansion deformation, impurity, and vibration or a combination of force-induced tensile deformation, impurity, and vibration. Similarly, the formation of the expectation-type accuracy fluctuation model ④ can occur due to a combination of thermal contraction deformation, wear, and vibration or a

combination of force-induced compressive deformation, wear, and vibration.

Again, take the expectation of the X-direction KE of the MAU as an example. According to equation (2), the expectation of the X-direction KE of the MAU is

$$\mu_X = \mu_{IX} + \mu_{AX} + \mu_{GX}. \tag{5}$$

When the MAU experiences an expectation-type accuracy fluctuation, the expectation of the X-direction KE satisfies equation (6).

$$\begin{aligned}\mu'_X = \mu_X + \Delta\mu_X = (\mu_{IX} + \Delta\mu_{IX}) + (\mu_{AX} + \Delta\mu_{AX}) \\ + (\mu_{GX} + \Delta\mu_{GX})\end{aligned} \tag{6}$$

where $\Delta\mu_X$, $\Delta\mu_{IX}$, $\Delta\mu_{AX}$ and $\Delta\mu_{GX}$ respectively represent the fluctuation amounts of the expectation of the X-direction KE, IE, AE and GE when the MAU fluctuates.

(3) Variance-type accuracy fluctuation model

The variance-type accuracy fluctuation model refers to a model where the limit deviation and expectation of the KE distribution of the MAU in CNC machine tools remain unchanged, and only the variance changes. Obviously, the variance-type accuracy fluctuation means the KE is distributed 'equally' on both sides of the expectation, bounded by the upper and lower limit deviations, with only non-characteristic peaks and troughs changing, as shown in figure 6(c).

In figure 6(c), there are many combinations of causes for fluctuation that form a variance-type accuracy fluctuation model, such as the combination of wear and vibration, deformation and vibration, or wear, deformation and vibration.

Also, take the variance of the X-direction KE of the MAU as an example. According to equation (2), the variance of the X-direction KE of the MAU is

$$\sigma_X^2 = \sigma_{IX}^2 + \sigma_{AX}^2 + \sigma_{GX}^2. \tag{7}$$

When the MAU experiences a variance-type accuracy fluctuation, the variance of the X-direction KE satisfies equation (8).

$$\sigma_X'^2 = \xi_X^2\sigma_X^2 = \xi_{IX}^2\sigma_{IX}^2 + \xi_{AX}^2\sigma_{AX}^2 + \xi_{GX}^2\sigma_{GX}^2 \tag{8}$$

where ξ_X^2, ξ_{IX}^2, ξ_{AX}^2 and ξ_{GX}^2 respectively represent the fluctuation factors of the variance of the X-direction KE, IE, AE and GE when the MAU fluctuates.

(4) Composite-type accuracy fluctuation model

As noted, the deviation-type, expectation-type, and variance-type accuracy fluctuation models each require specific conditions related to factors such as wear, impurity, deformation, and vibration. In fact, these factors are typically randomly interwoven, collectively affecting the MAU. This results in composite-type accuracy fluctuation, characterized by at least two concurrent changes among the deviation, expectation, and variance of the KE. The most common form of such fluctuation involves simultaneous changes in deviation, expectation, and variance. Thus, this model is adopted to explain composite-type accuracy fluctuation.

Similarly, take the X-direction KE of the MAU as an example. According to equations (4), (6) and (8), the KE of the model should satisfy equation (9).

$$\begin{cases} KE'_X \sim N\left(\mu'_X, \sigma_X'^2\right) \\ T'_{XL} \le KE'_X \le T'_{XU} \end{cases}. \tag{9}$$

4. Evaluation indices of accuracy stability for MA units in CNC machine tools

The preceding section analyzed the typical accuracy fluctuation models of the MAU. It is evident that both single-type and composite-type models indicate that changes in the KE are inevitably accompanied by shifts in characteristic parameters, which can be traced to the typical causes of accuracy fluctuation. Changes in the characteristic parameters of geometric feature errors and AE for the MAU are illustrated in figure 7. Notably, changes induced by certain factors require analysis in conjunction with actual geometric characteristics and are thus not marked in figure 7.

The following takes an MAU in the severe wear stage as an example, which experiences 'pit-digging' wear. It is assumed that large impurity particles (with volume exceeding the trough volume of the fitting surface) enter the mating surfaces of MAU parts; meanwhile, a heat source induces overall expansion and deformation of MAU components, and vibration causes dynamic mating parts to oscillate. The fluctuation law of the MA kinematic accuracy under the combined effect of these typical causes is illustrated in figure 8.

As shown in figure 8, under the combined influence of typical CNC machine tool accuracy fluctuation causes, the expectation, variance, and upper/lower limit deviations of the MAU's GE and AE distributions change accordingly. Affected by these errors, the four key parameters of the KE also fluctuate. Based on the MAU's accuracy fluctuation law in CNC machine tools, the MA's kinematic accuracy fluctuation curve is derived, as shown in figure 9. Figure 9 reveals that expectation, variance, upper limit deviation, and lower limit deviation all fluctuate to varying degrees. Consequently, the MA's accuracy fluctuation follows a four-parameter distribution—i.e. the three-dimensional fluctuation of a truncated normal distribution—rather than the traditional single fluctuation of expectation.

In figure 9, $f(KE_\mu, t)$, $f(\sigma, t)$, $f(KE_U, t)$ and $f(KE_L, t)$ respectively represent the fluctuation curves of the expectation, standard deviation, upper limit deviation, and lower limit deviation of the KE of the MAU. Therefore, according to the changing laws of these four curves, accuracy fluctuation rate (AFR), accuracy variation rate (AVR), accuracy variation coefficient (AVC) and accuracy stability coefficient (ASC) are proposed to describe the changing characteristics of the KE of the MAU in CNC machine tools.

AFR characterize the changing rate of the expectation of the KE of the MAU over time. Then the AFR can be expressed as

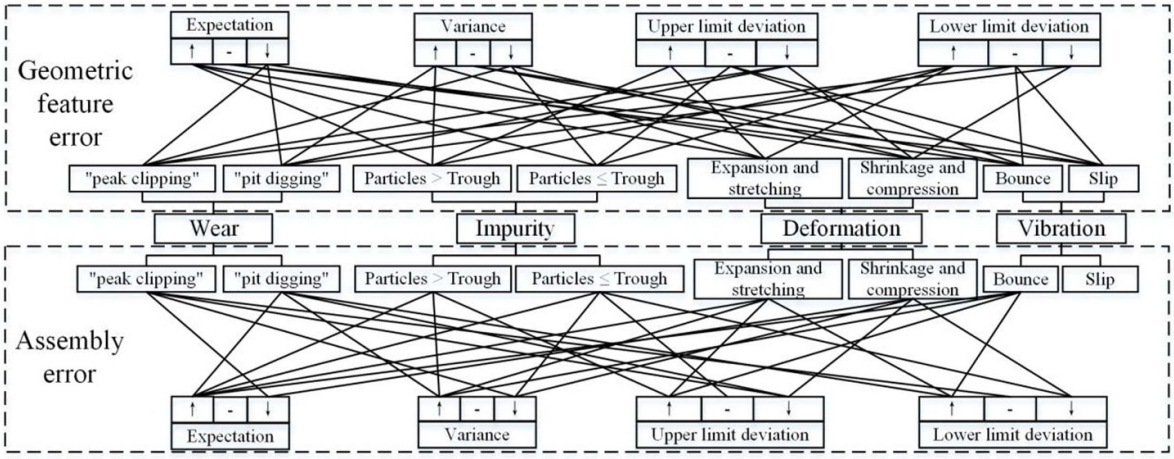


Figure 7. Changes in the characteristic parameters of the geometric feature errors and AE.

$$\mathrm{AFR} = \frac{\mathrm{d}f(KE_{\mu}, t)}{\mathrm{d}t}. \tag{10}$$

In equation (10), AFR indicates the degree of fluctuation of the expectation of the KE of the MAU per unit of time. Obviously, the larger the absolute value of the AVR, the greater the changing range of the expectation of the KE of the MAU, that is, the greater the degree of accuracy fluctuation.

AVR represents the change in the standard deviation of the KE of the MAU over time. Then the AVR can be expressed as

$$\mathrm{AVR} = \frac{\mathrm{d}f(\sigma, t)}{\mathrm{d}t}. \tag{11}$$

In equation (11), AVR represents the degree of fluctuation of the standard deviation of the KE of the MAU per unit time. Clearly, the larger the absolute value of the AVR, the greater the degree of discreteness of the KE of the MAU; that is, the greater the degree of accuracy fluctuation.

AVC characterize the degree of concentration of the KE of the MAU. It can be expressed as

$$\mathrm{AVC} = \frac{\sigma}{\mu} = \frac{f(\sigma, t)}{f(\mathrm{KE}_{\mu}, t)} | t = T. \tag{12}$$

In equation (12), AVC is the ratio of the standard deviation to the expectation used to measure the relative fluctuation of the KE of the MAU. Obviously, the smaller the absolute value of the AVC, the higher the concentration of the KE of the MAU.

ASC represents the degree of fluctuation of the KE of the MAU. It can be expressed as

$$\mathrm{ASC} = \frac{\mathrm{KE_U} - \mathrm{KE_L}}{\sigma} = \frac{f(\mathrm{KE_U}, t)\,|t = T - f(\mathrm{KE_L}, t)|t = T}{f(\sigma, t)\,|t = T}. \tag{13}$$

In equation (13), ASC is the ratio of the difference between the upper and lower limit deviations to the standard deviation, which is used to measure the stability of the accuracy of the MA. Clearly, the larger the ASC, the smaller the degree of fluctuation of the KE of the MAU; that is, the better the stability of the accuracy of the MA.

Due to the similarity between the calculation parameters of the accuracy stability coefficient ASC and the process capability index, a quantitative evaluation index for the accuracy stability coefficient ASC is provided based on the evaluation index of the process capability index [2]. General provisions:

When $\mathrm{ASC} < 6$, it means that the stability of accuracy of the MA cannot meet the requirements, that is, the degree of fluctuation of the KE of the MAU exceeds the specified range.

When $6 \leq \mathrm{ASC} < 8$, it means that the stability of accuracy of the MA basically meets the requirements, but the degree of fluctuation of the KE of the MAU is slightly larger.

When $8 \leq \mathrm{ASC} < 10$, it means that the stability of accuracy of the MA is better, and the degree of fluctuation of the KE of the MAU is small.

When $10 \leq \mathrm{ASC}$, it means that the stability of accuracy of the MA is ideal, and the degree of fluctuation of the KE of the MAU is much smaller.

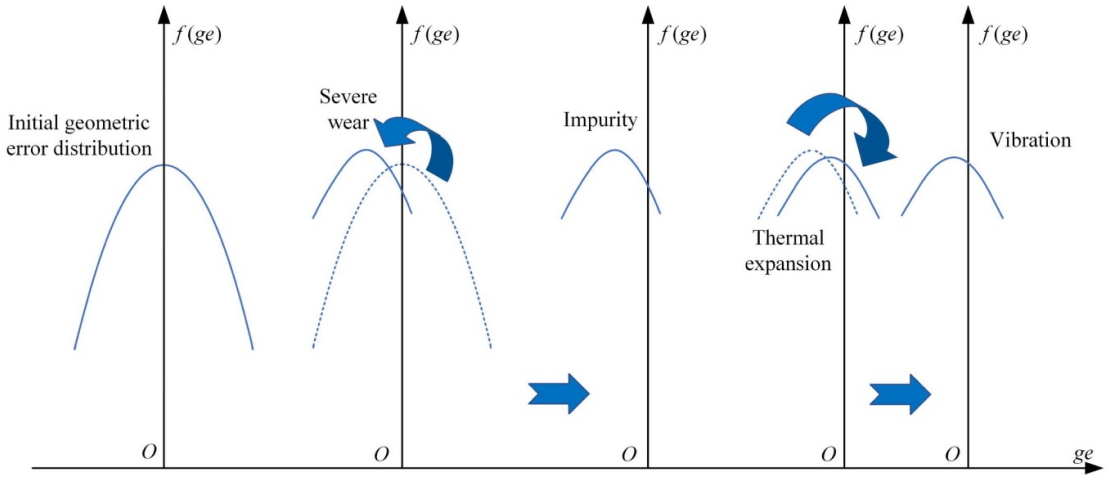
5. Comprehensive evaluation of accuracy stability of the MA in CNC machine tools

Section 4 has proposed relevant evaluation indices for the accuracy stability of the MA in CNC machine tools, which can quantitatively characterize the accuracy fluctuation of the MA. While a comprehensive consideration of these indices enables reasonable judgments on MA accuracy stability, a single integrated index is introduced here for intuitive understanding and expression: the accuracy stability index (ASI), which vividly reflects the accuracy stability of the MA.

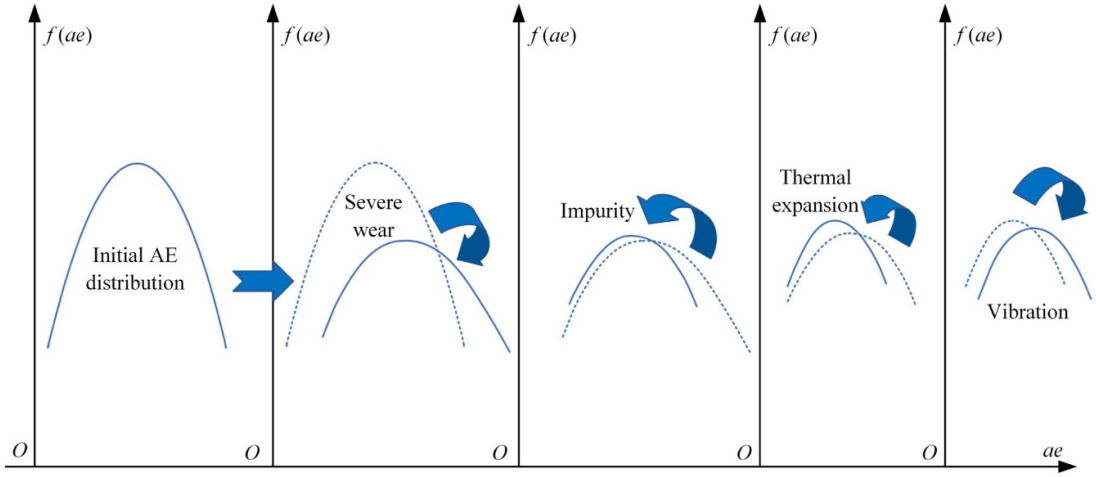
ASI is a measurement method to gauge the fluctuation level of the KE of the MAU. It can be used to comprehensively evaluate the accuracy stability of the MAU in CNC machine tools. Calculated as follows

$$\mathrm{ASI} = \mathrm{ASC} \cdot \mathrm{AVC}^2. \tag{14}$$

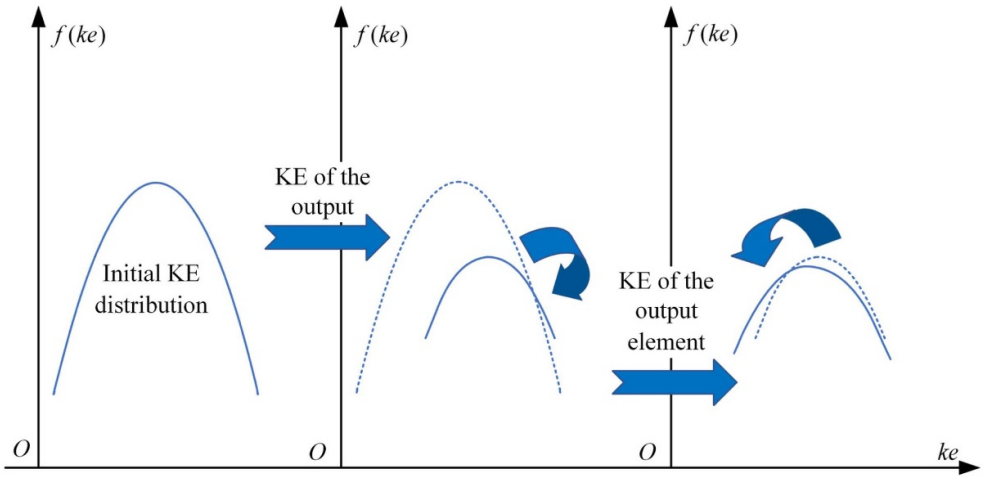
From equation (14), the ASI is jointly determined by the ASC and AVC, which is a comprehensive representation of the fluctuation results of the expectation, variance, upper limit deviation, and lower limit deviation of



(a) Geometric error



(b) Assembly error



(c) Kinematic error

Figure 8. Fluctuation law of the kinematic accuracy of the MA.

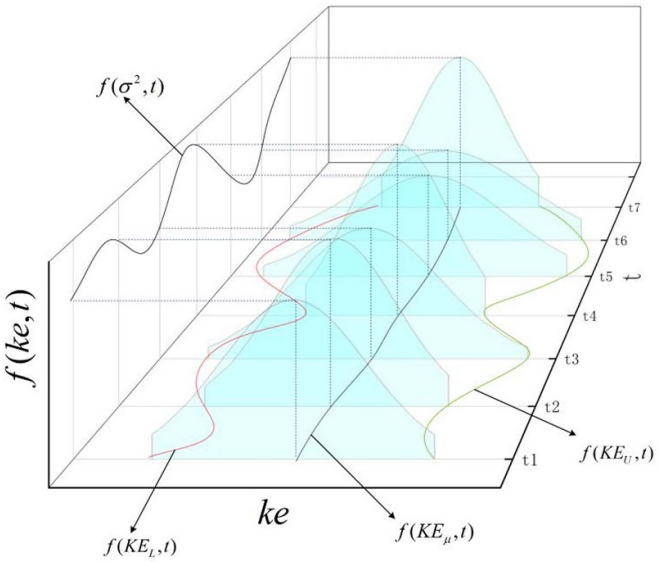


Figure 9. Accuracy fluctuation curve of the MA.

the KE of the MAU, fully reflecting the situation of accuracy fluctuation. Therefore, the ASI can be used as a comprehensive evaluation index of accuracy stability for the MAU.

Obviously, the smaller the value of the ASI, the less the fluctuation of the accuracy of the MA, and the greater the ability of the MAU to maintain the accuracy stable. When the fluctuation of the MA reaches a certain level, the accuracy of the output part of the MAU cannot meet its performance requirements; that is, the ASI of the MAU should not be less than a certain value so that the accuracy of the MA can meet the performance requirements for the normal production of CNC machine tools. Assuming that the threshold value of ASI for the normal operation of the MA is ψ, the criterion for judging the abnormality of the accuracy of the MA can be derived as

$$\mathrm{ASI} \geq \psi . \tag{15}$$

When the ASI exceeds ψ, the MA accuracy is deemed abnormal. The impact of such abnormality on CNC machine tool performance depends on product quality requirements. Given the significant differences in accuracy demands among high-, medium-, and low-grade CNC machine tools, the ASI threshold should be set accordingly, and different ASI levels can be defined based on the severity of damage caused by the accuracy anomaly, as shown in figure 10.

In figure 10, damage level I indicates that the accuracy abnormality directly destroys the MAU; level II indicates severe vibration and noise in the MAU, with accuracy failing to meet performance requirements; level III indicates mild vibration and noise in the MAU, resulting in unstable performance; and level IV indicates no noticeable vibration or noise yet, though occasional abnormal sounds may occur.

For high-accuracy CNC machines, even minor accuracy fluctuations can render machining quality unqualified before abnormal sounds emerge in the MAU. When the MAU's ASI

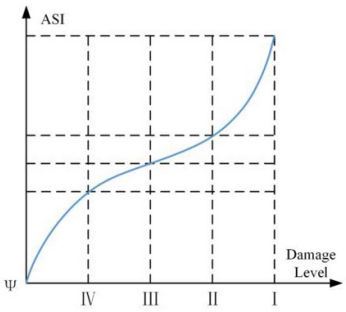


Figure 10. Matrix diagram of damage of accuracy abnormality of the MA.

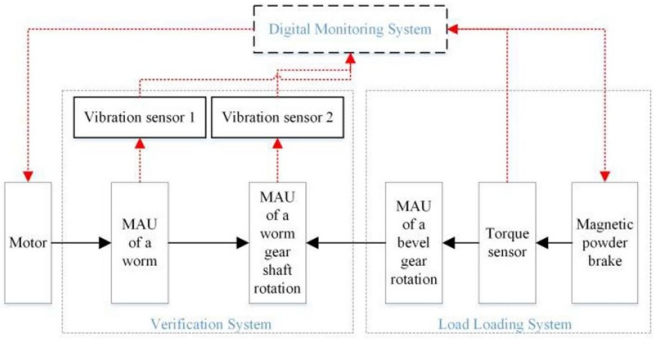


Figure 11. Design scheme of the test bench.

approaches Ψ, maintenance plans should be formulated to prevent damage escalation, which could ultimately lead to serious accidents or economic losses.

6. Case analysis

To verify the correctness and practical applicability of the proposed accuracy stability evaluation system for the MAU in CNC machine tools, a dedicated test bench for accuracy fluctuation law verification—based on a worm-gear set—was designed and built. The test bench scheme and overall view are shown in figures 11 and 12. Its core components consist primarily of two rotating MAUs, with auxiliary systems including a load application system and a digital monitoring system.

The design scheme works as follows: a motor drives the worm rotation MAU, which then rotates the worm gear shaft rotation MAU via worm-gear meshing. The worm gear shaft end connects to a bevel gear rotation MAU through bevel gears, transmitting the load torque from the magnetic powder brake to the worm gear shaft rotation MAU. Vibration signals from the worm and worm gear shaft are acquired using vibration sensors; based on the sensor operating principle [16], these signals are used to characterize the MA fluctuations in the *X, Y*, and *Z* directions. The vibration sensors were mounted on the housings of the worm and worm gear shaft rotation MAUs, respectively, using magnetic bases. Two orthogonal sensors were placed on each housing to capture vibrations in the *X* and *Y* directions; a third sensor was not used due to space constraints. The digital monitoring system consisted



Figure 12. Overall view of the test bench.

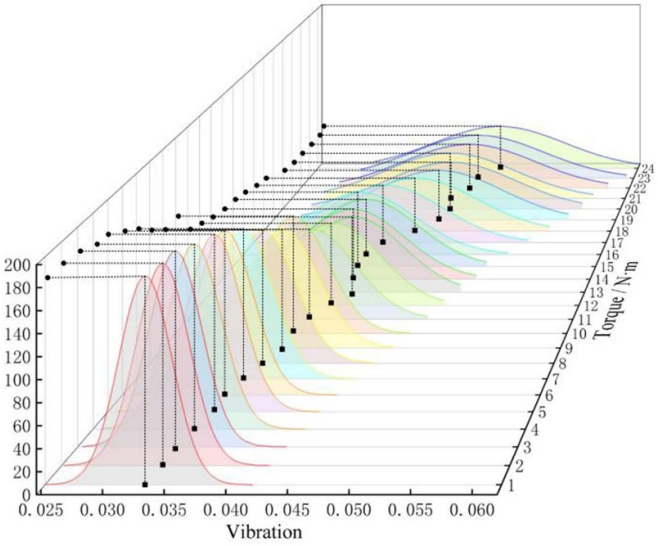


Figure 13. Vibration fluctuation law of the MAU of the worm gear rotation.

of a NI PXIe-1073 chassis with a PXIe-4499 data acquisition module (sampling rate 51.2 kHz per channel, 24-bit resolution). For each torque condition, 10 consecutive samples of 6 s each were recorded per minute, and the root-mean-square value of the vibration acceleration in the Y direction was extracted as the proxy for KE of the worm gear rotation MAU.

The motor speed is kept constant via the control system, while the magnetic powder brake varies the load torque from 0 to 24 N m in 1 N m increments, with each state maintained for 4 min. Multiple consecutive tests are conducted, during which the vibration sensor samples 10 times per minute. The selected torque range covers typical cutting loads encountered by a worm gear drive in medium-duty CNC rotary tables. The upper bound 24 N m corresponds to the rated torque of the magnetic powder brake; The lower bound 1 N m ensures negligible load to establish a baseline.

After data processing, Y-direction vibration values of the worm gear rotation MAU under 1–24 N m varying torque were selected to plot its accuracy fluctuation law, as shown in figure 13. Given that ∼2400 vibration data points were collected over 4 min for each torque, the time axis in the accuracy fluctuation graph is replaced with torque values.

Based on figure 13, the peaks and endpoints in the graph are projected onto the coordinate planes respectively, and polynomial fitting is applied to plot the fluctuation curves of the expectation, standard deviation, upper limit deviation, and lower limit deviation for the worm gear rotation MAU, $f(\Delta_\mu, T)$, $f(\Delta_\sigma, T)$, $f(\Delta_{\mathrm{U}}, T)$ and $f(\Delta_{\mathrm{L}}, T)$ as shown in figure 14.

From figure 14, the fitting equation of each characteristic fitting curve can be obtained

$$\begin{cases} \Delta_\mu = 3\times10^{-7}T^3 + 3\times10^{-6}T^2 + 0.0003T + 0.0323 \\ \Delta_\sigma = \frac{1}{\sqrt{2\pi}\,(-0.0027T^4+0.152T^3-2.6384T^2+7.2434T+177.1)} \\ \Delta_{\mathrm{U}} = -6\times10^{-7}T^3 + 4\times10^{-5}T^2 + 0.0002T + 0.0415 \\ \Delta_{\mathrm{L}} = 1\times10^{-6}T^3 - 4\times10^{-5}T^2 + 0.0005T + 0.024 \end{cases} \tag{16}$$

From equations (10)–(13), the accuracy stability evaluation indices of the MA of the worm gear rotation at each torque change can be calculated, as shown in table 2.

Table 2 shows that as torque increases, the AFR, AVR, and AVC of the worm gear rotation MAU gradually increase, all indicating declining accuracy stability of the MA. While AVR better reflects the overall accuracy stability of the MAU compared to AVC and AFR, it fails to capture the characteristics of the MAU's accuracy fluctuation.

As interference increases, the ASC of the worm gear rotation MAU gradually decreases. At 1 N · m torque, the ASC is already below 8, indicating poor accuracy stability of the worm gear rotation MAU—i.e. weak resistance to accuracy fluctuation. When torque exceeds 9 N · m, the ASC drops below 6, meaning the MAU's fluctuation degree exceeds its capacity to maintain normal rotation, rendering it unable to output correct motion and power.

From equation (14), the ASI of the worm gear rotation MAU can be calculated, as shown in table 3.

Table 3 shows that ASI increases with interference, indicating declining accuracy stability. Combined with AFR and AVR, the threshold ψ for normal operation of the worm gear rotation MAU is set at 0.1. That is, when the ASI is greater than 0.1, it can be determined that the accuracy of the MAU is abnormal. Thus, based on ASI, the MAU's accuracy is deemed abnormal when torque exceeds 14 N · m.

Compared with the ASC, although both can give quantitative values, ASI represents the overall characteristics of the

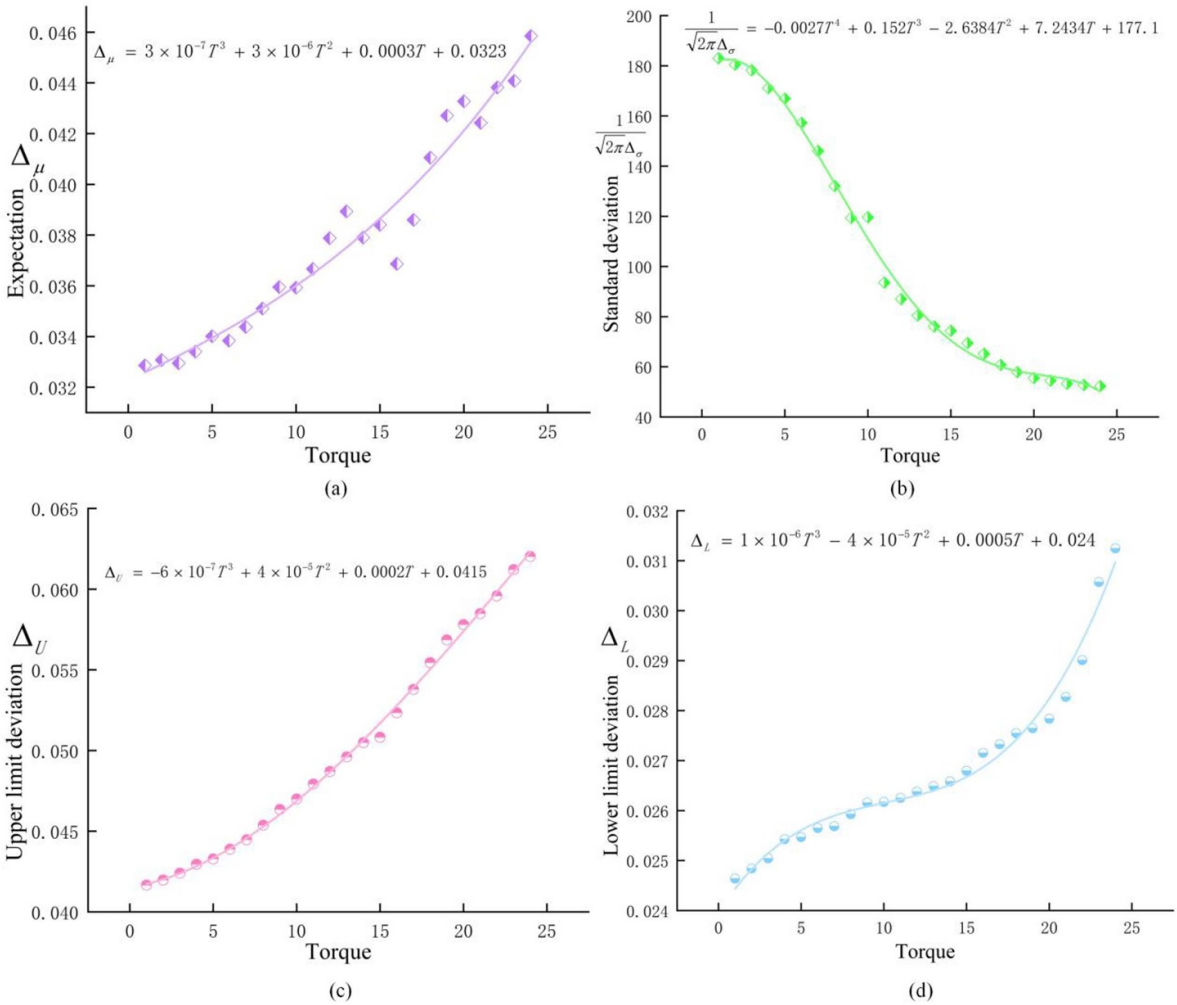


Figure 14. Fitting curves of fluctuation characteristics. (a) Expectation, (b) standard deviation, (c) upper limit deviation, (c) lower limit deviation.

Table 2. Evaluation indices.

Torque	1	2	3	4	5	6
AFR	0.0003069	0.0003156	0.0003261	0.0003384	0.0003525	0.0003684
AVR	-2.91×10^{-05}	1.89×10^{-05}	5.947×10^{-05}	9.688×10^{-05}	0.0001337	0.0001718
AVC	0.06729	0.06652	0.06707	0.06874	0.07144	0.07514
ASC	7.8762	7.8589	7.7506	7.5745	7.3472	7.0805
Torque	7	8	9	10	11	12
AFR	0.0003861	0.0004056	0.0004269	0.00045	0.0004749	0.0005016
AVR	0.0002122	0.0002554	0.0003014	0.0003492	0.0003965	0.0004396
AVC	0.07986	0.08562	0.09246	0.1004	0.1094	0.1193
ASC	6.7838	6.4656	6.1344	5.7991	5.4690	5.1541
Torque	13	14	15	16	17	18
AFR	0.0005301	0.0005604	0.0005925	0.0006264	0.0006621	0.0006996
AVR	0.0004734	0.0004920	0.0004907	0.0004679	0.0004283	0.0003837
AVC	0.1299	0.1408	0.1515	0.1614	0.1701	0.1773
ASC	4.8639	4.6071	4.3907	4.2187	4.0912	4.0032
Torque	19	20	21	22	23	24
AFR	0.0007389	0.00078	0.0008229	0.0008676	0.0009141	0.0009624
AVR	0.0003523	0.0003571	0.0004271	0.0006059	0.0009825	0.001792
AVC	0.1831	0.1881	0.1936	0.2015	0.2148	0.2397
ASC	3.9437	3.8945	3.8294	3.7140	3.5049	3.1497

Table 3. ASI.

Torque	1	2	3	4	5	6
ASI	0.03566	0.03478	0.03486	0.03579	0.0375	0.03998
Torque	7	8	9	10	11	12
ASI	0.04326	0.0474	0.05244	0.05844	0.06542	0.07333
Torque	13	14	15	16	17	18
ASI	0.08205	0.09131	0.1008	0.1099	0.1184	0.1258
Torque	19	20	21	22	23	24
ASI	0.1322	0.1378	0.1436	0.1507	0.1617	0.181

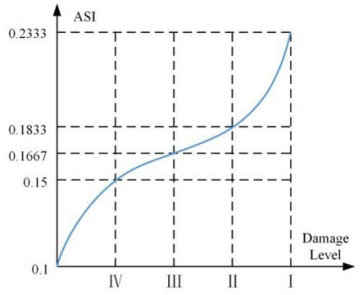


Figure 15. Matrix diagram of the damage of accuracy abnormality.

accuracy distribution, while ASC reflects more on its discreteness. ASI can more comprehensively represent the accuracy fluctuation level of the MA. If only the accuracy fluctuation of the MA needs to be judged, ASC can meet the requirements. However, if more detailed guidance is needed, ASI can only be used for evaluation. Next, ASI is used to determine the accuracy abnormality of the MAU of the worm gear rotation.

The damage matrix diagram for accuracy abnormalities of the worm gear rotation MAU is shown in figure 15. Based on the test bench's actual operation, the ASI for damage Level IV is set at 0.15, with corresponding ASI values for Levels III, II, and I derived sequentially.

As shown in figure 15, at 22 N · m and 23 N · m torque, the worm gear rotation MAU is at damage level III: significant MA accuracy fluctuation occurs, with noticeable vibration and noise from the test bench—consistent with level III descriptions. At 24 N · m torque, violent vibration and sharp noise emerge, and the MAU's accuracy clearly fails to meet normal operation requirements.

7. Conclusions

With the rapid development of the manufacturing industry, the quality of CNC machine tools has become increasingly critical, and accuracy stands as their core quality characteristic. However, the causes, mechanisms, and models of machine tool accuracy fluctuation are complex and diverse. Merely analyzing surface causes without exploring intrinsic formation mechanisms fails to address the problem fundamentally. To tackle this challenge, this paper proposes a universal analysis method based on MA theory, which clarifies accuracy fluctuation mechanisms and enables effective evaluation of accuracy stability. The main contributions of this work are summarized as follows:

(1) Based on the theory of the MA, this paper analyzes the accuracy fluctuation mechanisms under four key influencing factors and derives four corresponding typical accuracy fluctuation models. It ultimately clarifies the inherent accuracy fluctuation laws of MAUs in CNC machine tools.
(2) It establishes a set of accuracy stability evaluation indices for MAUs and a comprehensive evaluation system. The ASI, as the core comprehensive indicator, not only quantitatively measures the degree of the MAU accuracy fluctuation and intuitively reflects the fluctuation characteristics but also realizes the quantitative identification of the MAU accuracy abnormality levels.
(3) The proposed theory and analytical framework provide a theoretical reference for the research on other quality characteristics of CNC machine tools, expanding the application scope of MA theory in the field of CNC machine tool quality research.

Nevertheless, several challenges and future perspectives remain for practical implementation:

(1) Industrial integration challenges. Integrating the proposed indices (AFR, AVR, AVC, ASC, ASI) into existing CNC monitoring or predictive maintenance frameworks faces technical difficulties in real-time data acquisition, computational overhead, and standardized communication protocols. Future efforts should focus on lightweight algorithms and IoT-based platform compatibility.
(2) Extension to other quality characteristics. Applying this framework to thermal stability and dynamic stiffness of MAUs requires establishing cause-effect models for those characteristics, decoupling multi-factor interactions, and defining unified evaluation indices—representing key next-step research directions.
(3) Practical application and limitations. The ASI framework can be applied by pre-establishing threshold Ψ for specific MAU types and triggering abnormality alerts when ASI exceeds Ψ. However, current validation is limited

to worm-gear MAUs on a dedicated test bench, and the indices are sensitive to measurement conditions. Future validation should target multiple MAU types, long-term run-to-failure tests, and industrial case studies on actual CNC machine tools.

Data availability

The data will be available on request.

Funding

This work was supported by the National Natural Science Foundation of China (Grant Nos. [52275473] and [51835001]) and the Fundamental Research Funds for the Central Universities (No. 2025CDJZKZCQ-04).

Conflict of interest

The authors have no relevant financial or non-financial interests to disclose.

Author contributions

All authors contributed to the study conception and design. Jindong Xu: Conceptualization, Methodology, Investigation. Ke Tian: Investigation. Yan Ran: Supervision. The first draft of the manuscript was written by Yan Ran and all authors commented on previous versions of the manuscript. All authors read and approved the final manuscript.

Compliance with ethical standards

Research involving human participants and/or animals

Not applicable.

Informed consent

Written informed consent for publication of this paper was obtained from Chongqing University and all authors.

ORCID iD

Jindong Xu 0009-0000-6778-8152

References

[1] Ran Y and Lv Y 2026 Abnormality assessment of workpiece machining accuracy based on two-stage grey cloud model *China Mech. Eng.* **37** 383–9

[2] Liu P, Du Z, Feng X and Yang J 2020 Thermal error modeling and compensation of CNC machine tools based on workpiece dimensions *Mach. Des. Res.* **36** 122–125,131

[3] Chao X and Li Y 2026 Geometric errors and compensation technology of five-axis CNC machine tools *Rock Drilling Machinery and Pneumatic Tools* vol **52** pp 175–7

[4] Song L, Liu K, Cui Y, Chen H, Chen Y and Wang Y 2022 Time-varying error compensation for horizontal machining center based on mechanism-driven model *Acta Aeron. Astron. Sin.* **43** 493–501

[5] Mechta A, Slamani M, Zaoui M, Mayer R and Chatelain J-F 2022 Correlation assessment and modeling of intra-axis errors of prismatic axes for CNC machine tools *Int. J. Adv. Manuf. Technol.* **120** 5093–115

[6] Chen X, Jin X, Shang K and Zhang Z J 2019 Entropy-based method to evaluate contact-pressure distribution for assembly-accuracy stability prediction *Entropy* **21** 322

[7] He K, Hong H, Jiang G and Gu H 2020 Analysis of assembly error effect on stability accuracy of unmanned aerial vehicle photoelectric detection system *Appl. Sci.* **10** 2311

[8] Zhou J 2018 Stability analysis of 16 meter vertical lathe accuracy and its impact on machining accuracy *Technology Markets* **25** 83–5

[9] Li Y, Zhang X, Ran Y, Zhang G and Wang Y 2020 Research on meta-action decomposition and meta-action unit modeling technology for electromechanical product *Qual. Reliab. Eng. Int.* **36** 268–84

[10] Li Y, Zhang X, Ran Y and Zhang G 2021 Reliability modeling and analysis for CNC machine tool based on meta-action *Qual. Reliab. Eng. Int.* **37** 1451–67

[11] Chen Y, Ran Y, Wang Z, Li X, Yang X and Zhang G 2021 Meta-action reliability-based mechanical product optimization design under uncertainty environment *Eng. Appl. Artif. Intell.* **100** 1–12

[12] Yang X, Ran Y, Zhang G, Wang H, Mu Z and Zhi S 2022 A digital twin-driven hybrid approach for the prediction of performance degradation in transmission unit of CNC machine tool *Robot. Comput. Integr. Manuf.* **73** 102230

[13] Zhang Z, Xie G, Shao Z and Gosselin C 2022 Kinematic calibration of cable-driven parallel robots considering the pulley kinematics *Mech. Mach. Theory* **169** 104648

[14] Zeng X, Xiong W, Zhang H, Li Y, Yuan S and Jin Z 2023 Research on the consistency model of roundness error in journal cylindrical grinding with random parameters *Precis. Eng.* **82** 270–80

[15] Swain B, Bhuyan S, Behera R, Mohapatra S S and Behera A 2020 Wear: a serious problem in industry *Tribology in Materials and Manufacturing-Wear, Friction and Lubrication* (IntechOpen)

[16] Mian T, Choudhary A and Fatima S 2022 A sensor fusion based approach for bearing fault diagnosis of rotating machine *Proc. Inst. Mech. Eng. O* **236** 661–75



Jindong Xu graduated with a Bachelor's degree from the China University of Mining and Technology and is currently studying at Chongqing University.



Yan Ran received MS and PhD degrees in mechanical engineering from Chongqing University, Chongqing, China, in 2012 and 2016, respectively. She is currently an associate professor and a doctoral supervisor at Chongqing University, a fixed researcher at the State Key Laboratory of Mechanical Transmission for Advanced Equipment, Chongqing University, a committee member of the Chongqing Science and Technology Association and a vice president of Chongqing Engineering Graphics Society, etc. Their research interests include CNC machine tools reliability technology and electromechanical product quality engineering. They have hosted and joined in almost 30 projects, published more than 100 academic papers, 24 invention patents and six copyrights of computer software.



Ke Tian graduated with a Master's degree from Chongqing University and is currently working at the Southwest Institute of Technical Physics.